ISBN: 978-3-95450-214-1 ISSN: 2673-5490 doi:10.18429/JACoW-IPAC2021-TUPAB285

BROADBAND IMAGING OF COHERENT RADIATION AS A SINGLE-SHOT BUNCH LENGTH MONITOR WITH FEMTOSECOND RESOLUTION

J. Wolfenden*, E. Kukstas, R. Fiorito, C. P. Welsch
University of Liverpool/Cockcroft Institute, Liverpool, UK
B. Kyle, E. Mansten, M. Brandin, S. Thorin, MAX IV, Lund, Sweden
T. H. Pacey, ASTeC, Warrington, UK

Abstract

Bunch length measurements with femtosecond resolution are a key component in the optimisation of beam quality in FELs, storage rings, and plasma-based accelerators. This contribution presents the development of a novel single-shot bunch length monitor with femtosecond resolution, based on broadband imaging of the spatial distribution of emitted coherent radiation. The technique can be applied to many radiation sources; in this study the focus is coherent transition radiation (CTR) at the MAX IV Short Pulse Facility (SPF). Bunch lengths of interest at this facility are <100 fs FWHM; therefore the CTR is in the THz to Far-IR range. To this end, a THz imaging system has been developed, utilising high resistivity float zone silicon lenses and a pyroelectric camera; building upon previous results where single-shot compression monitoring was achieved. This contribution presents simulations of this new CTR imaging system to demonstrate the synchrotron radiation mitigation and imaging capability provided, alongside initial measurements and a bunch length fitting algorithm, capable of shot-to-shot operation. A new machine learning analysis method is also discussed.

INTRODUCTION

Ultra-short bunch lengths in the <100 fs range are becoming more commonplace in the accelerator sector. Free electron lasers are leading this push to shorter bunches with the many applications afforded by the short x-ray pulses produced. However, longitudinal diagnostics in this regime are limited to a handful of solutions. These systems are mostly interferometric [1], spectroscopic [2], or electro-optical [3]. Each have their strengths and weaknesses, but generally there is a compromise between longitudinal profile resolution, number of shots required, and ease of application. This proceedings will describe a new longitudinal profile monitor which is simple to operate on a shot-to-shot basis, and provides a fs-resolution measurement to the bunch profile width and features - beaten only by a full spectroscopic reconstruction. As this is an imaging method no phase information is collected, therefore the full profile cannot be reconstructed; however features of the profile can be measured given a predetermined profile shape (e.g. Gaussian, double-Gaussian, etc.). This new system is based upon broadband imaging of coherent radiation. Work presented here will focus on the application of this technique to transition radiation (TR) but in principle other non-interceptive radiation sources, e.g. synchrotron radiation (SR), can be used.

TR is produced when the electric field of a charged particle traverses the boundary between two different dielectric constants [4]. TR has a broadband spectral distribution, of which a specific bandwidth is typically studied. If this bandwidth contains wavelengths comparable to or exceeding the bunch length of the source bunch, the radiation will be coherent, hence CTR.

BROADBAND IMAGING

Previous studies have shown that images produced by this broadband imaging methodology are dependent upon longitudinal bunch properties [5–7]. This imaging technique is based upon how a coherent image is constructed. In this short bunch regime the particles of interest are typically electrons, therefore this shall be the assumed source of the CTR moving forward. The image, I^i_{bunch}, for an electron bunch is calculated using the image from a single electron at a single frequency, I^i_e, multiplied by the longitudinal bunch form factor, F_z, integrated over the applicable broadband bandwidth, $\Delta\omega$ [6, 8, 9]. The theoretical calculation for a CTR image is:

$$\frac{dI^i_{bunch}}{dr} \approx N_e^2 \int_{\Delta\omega} \frac{d^2 I^i_e}{d\omega dr} \left|F_z\left(\rho\left(z\right),\omega\right)\right|^2 d\omega, \quad (1)$$

where r is the spatial position on the image plane, N_e is the number of electrons in the bunch, $\rho(z)$ is the longitudinal bunch profile, ω is the frequency of the emitted TR, and F_z is the longitudinal form factor. Equation (1) assumes a large N_e, to neglect incoherent contributions. It also assumes a transverse size, σ_r, which is $< \gamma\lambda/2\pi$, where γ is the Lorentz factor of the particle and $\lambda = 2\pi c/\omega$. The transverse form factor, F_r, will then be ≈ 1 and only F_z needs to be accounted for; assuming $F_r \approx 1$ for a 1 GeV electron beam at 10 THz, σ_r must be <9 mm - a valid assumption for modern accelerators. Equation (1) demonstrates that the image produced by the integration over $\Delta\omega$ is the summation of the individual spectral images, modulated by F_z. Therefore, if $\Delta\omega$ is chosen to capture the spectral range over which F_z varies for a specific bunch profile variation, any changes in $\rho(z)$ will be apparent in the image produced.

The theory detailed above would work equally well for angular distributions as it does for spatial imaging. However a significant disadvantage of using the angular distribution is that the detector is typically placed in the focal plane of the optical element of the imaging system. This configuration

* joseph.wolfenden@cockcroft.ac.uk

ISBN: 978-3-95450-214-1 ISSN: 2673-5490 doi:10.18429/JACoW-IPAC2021-TUPAB285

focuses all rays from the source plane with specific angular properties, as well as upstream sources sharing those same properties, to the same spatial position in the focal plane. In this configuration, when multiple radiation sources are within the coherence length, $L = \gamma^2 \lambda$, of one another they can interfere and distort the expected angular distribution of a single source [10, 11]. At coherent wavelengths it becomes impossible in practise to separate two radiation sources by a sufficiently large distance, as often $L >> 10$ m. Therefore interference occurs amongst the various upstream sources, and the resulting distribution can become incompatible with diagnostic requirements. For spatial imaging, these upstream sources are still collected, but as the detector is placed in the image plane rather than the focal plane, these sources become a de-focused, defuse background.

DIAGNOSTIC DEVELOPMENT

Previous work has developed and tested several iterations of broadband imaging systems [6, 7]. These systems have been proof of concept designs, with a focus of proving the methodology. Building on this, the focus of current work is to develop an operational diagnostic.

To achieve this two main improvements have been carried out. The first was an improved detector. Previous detectors have all been pyroelectric detectors of different formats and specifications; these were either a large single pixel which was scanned across the image plane, or a 1D linear array. The new detector for this system is a Pyrocam [12]. This is a 2D array of pyroelectric crystals, capable of providing high resolution, high broadband sensitivity, single-shot images.

The second improvement has been the development of an optimised imaging system. Previous systems had focused on ease of use to minimise potential sources of errors in the proof of concepts measurements, however this lead to several spectral “dead zones”in the broadband spectrum. This ultimately limited the achievable resolution for these systems. A new system has therefore been designed based on high resistivity float zone silicon (HRFZ Si), which has a very large window of transmission, but is opaque at optical wavelengths making alignment and focusing more difficult. The system contains a gold target, a HRFZ Si vacuum window, followed by a single plano-convex HRFZ Si lens.

The broadband imaging capability was simulated using Zemax OpticStudio [13]. The elements detailed above were positioned in a simple 2*f*-2*f* imaging setup (for simulation purposes), where *f* is the focal length of the lens, which was 100 mm in this instance. This imaging system was focused on a TR target tilted at 45° relative to the beam propagation direction. A simple schematic of the system is presented in Fig. 1. The ray diagram in Fig. 1a shows how the system will focus the TR radiation, while Fig. 1b shows how the rays from an upstream source, for example coherent SR (CSR), would behave. It is clear from the ray diagrams that any upstream source is going to be completely de-focused and rendered a low-level background to the main CTR image.

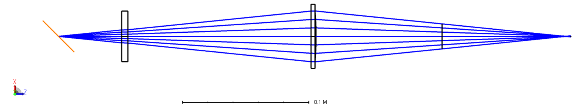

(a)

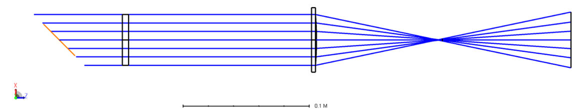

(b)

Figure 1: Single HRFZ Si lens imaging system in a 2*f*-2*f* setup imaging a TR target at 45°. Top: CTR ray diagram. Bottom: upstream source (e.g. CSR) ray diagram.

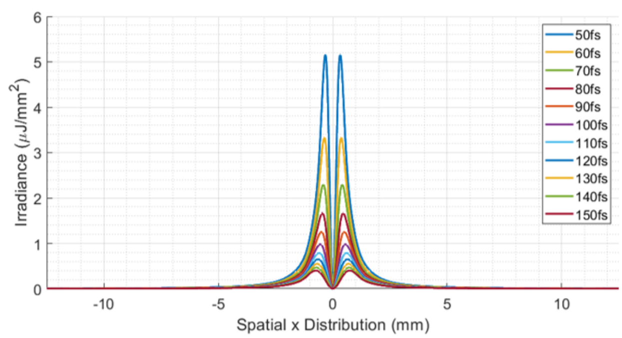

Figure 2: Example simulated CTR image profiles using the system shown in Fig. 1.

The performance of this system was simulated for a range of single Gaussian longitudinal profiles. Line scans of the images produced are presented in Fig. 2. The image profiles can be clearly seen to vary in intensity and width for a varying bunch length. Indeed this is the basis for the current analysis methodology. Figure 3 presents calibration curve which can be generated from these simulations. The basis for this is that a broadband CTR image of the electron bunch can be taken, then by comparing the peak-to-peak separation of this image to the curve, a FWHM bunch length for a Gaussian approximation of the bunch can be retrieved.

This system has now been installed at the MAX IV SPF (Lund, Sweden), as can be seen in Fig. 4, alongside the very first single-shot CTR test image. System benchmarking measurements shall be begin later this year.

NEURAL NETWORK ANALYSIS

As described in the previous section, current analysis distils the information contained in the broadband images into a single value of peak-to-peak width; this discards a large majority of the information within the image and assumes the longitudinal bunch profile is approximately Gaussian.

In recent years machine learning techniques, particularly neural networks (NN), have proven to be perfectly suited to this type of feature recognition problem. To utilise all useful information contained within an image, a new NN analysis

ISBN: 978-3-95450-214-1 ISSN: 2673-5490 doi:10.18429/JACoW-IPAC2021-TUPAB285

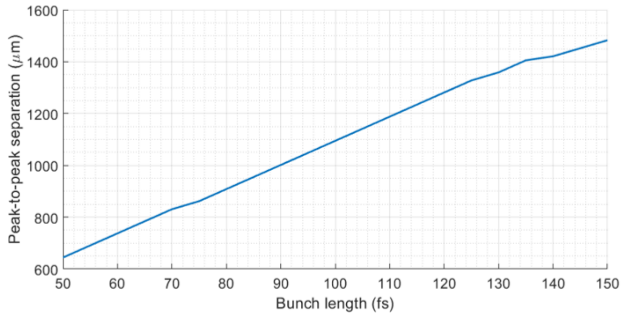

Figure 3: Typical analysis of the images presented in Fig. 2. CTR image width variation with bunch length.

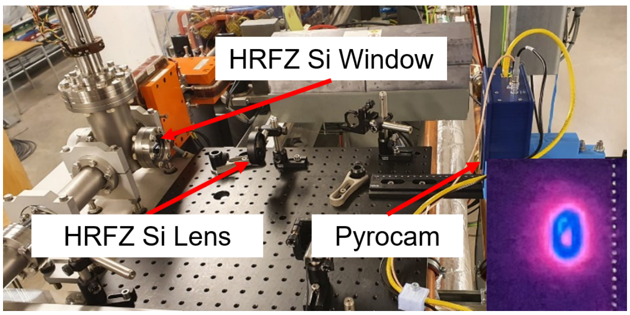

Figure 4: HRFZ Si system at the MAX IV SPF. Inset image is the first test image of CTR with the system.

method is being developed. As a first step, the simulations above were conducted using a double-Gaussian distribution. The six possible variables (2 widths, 2 amplitudes, and 2 offsets) were randomised within a range of parameters which could be expected from the MAX IV SPF.

100,000 of these images were used to train a feed-forward NN, with an 80:20 split between the training and validation sets. The network consisted of the pixel values of a 1D line profile of the CTR simulated images as inputs, three hidden layers, and the six double-Gaussian variables listed above as outputs. Each layer consisted of the following number of neurons: [256 (inputs), 256, 256, 256, 6 (outputs)]. Training used the Rectified Linear Unit as the activation function in all layers and the Adam optimiser. The network was trained for 10,000 epochs using a batch size of 100 and a learning rate of 1e-5. Open-source Keras and Tensorflow libraries were used to build and train the NN.

Figure 5 presents the results of the validation analysis on the model. The closer predicted values match the true values (black line), the better the model can predict the individual double-Gaussian parameters from a CTR image. Gaussian one had a fixed amplitude of 1 and an offset of 0 (not shown in Fig 5, predicted to 0.01% RMSE); Gaussian two associated parameters were then relative values. The results are extremely promising given the infancy of this work. The relative amplitude could be predicted to a 6.7% RMSE, the width of the first Gaussian to 1% RMSE, the width of the second Gaussian to 6.2% RMSE, and the relative offset to 17.2% RMSE. These first results are a significant improvement upon existing analysis. Work is now underway to extend this model to use the full 2D image, use more realistic bunch profiles, and apply this to measurements.

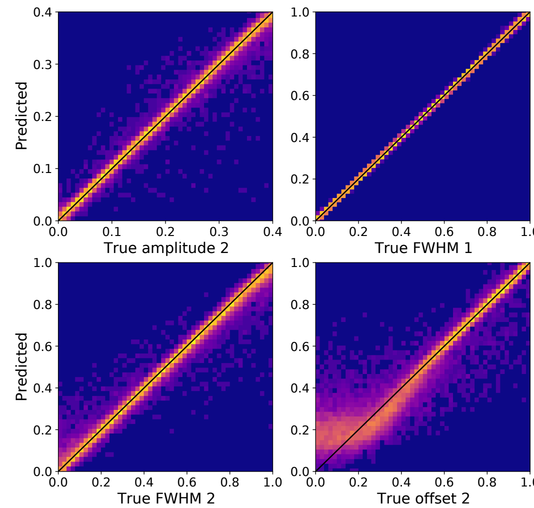

Figure 5: Initial validation results of the new neural network model for CTR image analysis.

DISCUSSION AND FUTURE PLANS

Described here is a bunch length monitor with the potential to provide shot-to-shot longitudinal profile information. Comparing images from MAX IV and simulations will be an important next step. Once initial commissioning of the system is complete, a full phase scan will be completed with corroborating measurements taken where possible for independent verification.

Following this, it would be straightforward to adapt this technology to image other, non-interceptive, radiation sources; this would make the technique non-invasive. A non-invasive single-shot method of measuring detailed longitudinal profile information would have accelerator applications. This is particularly the case for AWAKE (CERN, Switzerland) [14] where this system could be used to non-invasively monitor the longitudinal properties of the pre-injection, and the post-plasma accelerated electron beams. Alongside these efforts, further study of the contribution of transverse profile variations will be conducted. This work assumes a coherent transverse form factor, which cannot always be guaranteed; e.g. for CSR transverse beam size can play a larger role [7].

Work will continue to leverage machine learning techniques to increase the insight a single image can provide, building upon these promising first results.

ACKNOWLEDGEMENT

This work is supported by the AWAKE-UK project funded by STFC and the STFC Cockcroft core grant No. ST/G008248/1.

REFERENCES

[1] B. Schmidt, N. M. Lockmann, P. Schmüser, and S. Wesch, “Benchmarking coherent radiation spectroscopy as a tool for

ISBN: 978-3-95450-214-1 ISSN: 2673-5490 doi:10.18429/JACoW-IPAC2021-TUPAB285

high-resolution bunch shape reconstruction at free-electron lasers", *Phys. Rev. Accel. Beams*. vol. 23, p. 062801, Jun. 2020. doi:10.1103/PhysRevAccelBeams.23.062801

[2] A. Curcio *et al.*, "Noninvasive bunch length measurements exploiting Cherenkov diffraction radiation", *Phys. Rev. Accel. Beams*, vol. 23, p. 022802, Feb. 2020. doi:10.1103/PhysRevAccelBeams.23.022802

[3] A. Borysenko *et al.*, "Electron bunch shape measurements using electro-optical spectral decoding", *Physics Procedia*, vol. 77, pp. 3-8, Dec. 2015. doi:10.1016/j.phpro.2015.11.002

[4] M. Ter-Mikaelian, *High Energy Electromagnetic Processes in Condensed Media*", New York, USA: J. Wiley - Interscience, 1972.

[5] A. Shkvarunets, R. Fiorito, F. Mueller, and V. Schlott, "Diagnostics of the Waveform of Coherent Sub-mm Transition and Diffraction Radiation',' in *Proc. of DIPAC'07*, Venice, Italy, May 2007, paper WEPC21, p. 355.

[6] J. Wolfenden *et al.*, "Coherent Transition Radiation Spatial Imaging as a Bunch Length Monitor", in *Proc. 10th Int. Particle Accelerator Conf. (IPAC'19)*, Melbourne, Australia, May 2019, pp. 2713–2716. doi:10.18429/JACoW-IPAC2019-WEPGW095

[7] B. S. Kyle *et al.*, "Simulations and Measurements of Coherent Synchrotron Radiation at the MAX-IV Short Pulse Facility", in *Proc. 10th Int. Particle Accelerator Conf. (IPAC'19)*, Melbourne, Australia, May 2019, pp. 712–715. doi:10.18429/JACoW-IPAC2019-MOPRB061

[8] A. G. Shkvarunets and R. B. Fiorito, "Vector electromagnetic theory of transition and diffraction radiation with application to the measurement of longitudinal bunch size", *Phys. Rev. ST Accel. Beams*, vol. 11, no. 1, p. 012801, Jan. 2008. doi:10.1103/PhysRevSTAB.11.012801

[9] H. Loos, R. Akre, A. Brachmann, *et al.*, "Observations of Coherent Transition Radiation in the LCLS Linac", in *Proc. of FEL'08*, Gyeongju, Korea, Sep. 2008, paper THBAU01, p. 485.

[10] R. B. Fiorito, C. P. Welsch, A. G. Shkvarunets, C. Clarke, and A. Fisher, "Coherent Diffraction Radiation Imaging Methods to Measure RMS Bunch", in *Proc. of IBIC'16*, Barcelona, Spain, Sep. 2016, paper MOPG58, p. 198.

[11] R. Kieffer *et al.*, "Experimental Observation of "Shadowing" in Optical Transition Radiation", *Phys. Rev. Lett.*, vol. 120, no. 9, p. 094802, Feb. 2018. doi:10.1103/PhysRevLett.120.094802

[12] Pyrocam IIIHR Beam Profiling Camera by Ophir Optronics Solutions Ltd, www.ophiropt.com/laser--measurement/beam-profilers/products/Beam-Profiling/Camera-Profiling-with-BeamGage/Pyrocam-IIIHR

[13] Zemax OpticStudio, www.zemax.com/products/opticstudio

[14] E. Adli *et al.*, "Acceleration of electrons in the plasma wakefield of a proton bunch", *Nature*, vol. 561, pp. 363–367, Aug. 2018. doi:10.1038/s41586-018-0485-4